injections with lipidic-formulated synthetic miR-137. Moreover, immuno-blotting and -staining analysis of tumor tissue demonstrated that MCL-1was decreased in miR-137 overexpressing tumors compared to vector or delivery regent controls, as well as reduced Ki67 and increased Tunnel activities.

Conclusions: Our findings provide a proof-of-principle that lentivirus-based miR-137 or formulated synthetic miR-137 exerts therapeutic activity in preclinical models and support a framework for development of miR-137based treatment strategies in MM patients.

1923 Mining TCGA/COMSIC Data Reveals Rationale of Expanding Molecular/Genetic Testing to More Tumor Types: Implications for Personalized Oncology
H Zhong. Rutgers Robert Wood Johnson Medical School and Rutgers Cancer Institute of New Jersey, New Brunswick, NJ.
Background: Molecular/genetic testing has become a daily routine for pathology. Examples include PCR or FISH based analyses for ERBB2, BRAF, KRAS, EGFR, ALK and KIT. Results from the tests permit genomic classification of solid tumors and determine further managements. However, the current routine aims only to the most common tumor types based on prior translational studies. Large-scale cancer genomic data are gradually accumulated and are now available to research communities. Information from the large-scale well-maintained datasets may change our original concepts on cancer biology and genomics.
Design: TCGA cBioPortal for Cancer Genomics was used as an initial source of data mining. Tumors with genetic alterations of a specific gene in greater than 10% cases were recorded, arbitrarily designated as high-frequency alteration. COSMIC database was then queried if known activating mutation could be identified on the tumor.
Results: High-frequency genetic alteration on ERBB2 was demonstrated in four different carcinomas including breast and gastric carcinoma. Various tumors were shown to have high-frequency alteration on BRAF, KRAS and EGFR. ALK gene was altered in 10% cutaneous melanomas in addition 11.6% lung adenocarcinomas. Only one non-GIST tumor, glioblastoma, showed high-frequency KIT alteration while the majority were amplification. Below table shows examples.

Examples of Genetic Alterations in Solid Tumors

Gene	Tumor	Amplification (%)	Deletion (%)	Mutation (%)	Mixed Alterations (%)	Total Alterations (%)	Total Case Tested
ERBB2	Urothelial carcinoma	3.8		11.5	3.8	19.1	26
	Breast invasive carcinoma	13.6		1.4	0.1	15.1	760
	Endometrioid carcinoma	7.1		3.3		10.4	240
BRAF	Colorectal adenocarcinoma	0.5		10		10.5	221
	Lung adenocarcinoma	1.6		9.3	0.8	11.7	129
	Ovarian serous cystadenocarcinoma	10.6	0.3	0.6		11.5	311
	Cutaneous melanoma	0.9	0.4	45.2	6.1	52.6	228
	Thyroid carcinoma		0.3	58.9		59.2	319
EGFR	Glioblastoma	32.2		4.7	23.7	60.6	236
	Head & neck squamous cell carcinoma	8.6	0.3	3	1.7	13.6	302
	Lung adenocarcinoma	1.6		13.2	3.8	18.6	182
	Gastric adenocarcinoma	5.5	0.5	5		11	219

Conclusions: It is reasonable to extend PCR or FISH based analyses on all late-stage tumors with high-frequency of specific genetic alterations. At least, available immunohistochemistry should be performed to select candidates for further target genetic testing. By doing so, more cancer patients may access to personalized management before next-generation sequencing is adopted as a clinical routine.

Pediatric Pathology

1924 Fine Needle Aspiration Cytology in Pediatric Bone and Soft Tissue Spindle Cell Lesions
N Bures, L Pantanowitz, SE Monaco. University of Pittsburgh Medical Center, Pittsburgh, PA.
Background: Spindle cell lesions in children can be difficult to characterize by fine needle aspiration (FNA) given that the differential diagnosis varies by age, and includes reactive tumor-like lesions as well as benign and malignant neoplasms. The objective of this study is to assess the diagnostic utility of FNA in the diagnosis of spindle cell lesions in the pediatric population.
Design: Spindle cell lesions in patients 22 years of age or less were identified during the time period from 2006 to 2012. Cytology cases and surgical cases with a prior FNA were included. Patient demographics, FNA diagnosis, ancillary studies and available follow-up were investigated and correlated.
Results: A total of 18 cases were identified in patients ranging from 7 weeks to 22 years of age, including 9 males and 9 females. Lesions included 14 (78%) soft tissue and 4 (22%) bone lesions. Samples were acquired by image-guided FNA (9; 50%) or palpation guided FNA (9; 50%). Thirteen (72%) cases had corresponding histopathology. Four (22%) cases had sufficient material for ancillary studies. Table 1 shows the correlation of cytology adequacy and diagnoses with histological follow-up. No false positive diagnoses were identified.

Table 1. Cytohistological Correlation in Pediatric Spindle Cell Lesions

FNA Adequacy & Diagnosis	No. of cases (%)	No. with histological follow-up (%)	Histopathology Diagnosis Reactive	Histopathology Diagnosis Benign Neoplasm	Histopathology Diagnosis Malignant Neoplasm
Unsatisfactory, Non-Diagnostic	6 (33%)	3 (50%)	0	1 (hemangioma)	2 (osteosarcoma)
Less than optimal, Negative	2 (11%)	1 (50%)	0	1 (hemangioma)	0
Less than optimal, Atypical or Suspicious	2 (11%)	2 (100%)	0	1 (fibromatosis)	1 (epithelioid sarcoma)
Satisfactory, Atypical or Suspicious	3 (16%)	3 (100%)	0	3 (solid aneurysmal bone cyst, localized tenosynovial giant cell tumor, desmoplastic fibroma)	0
Satisfactory, Positive for Neoplasm	5 (28%)	4 (80%)	0	3 (schwannoma, ganglioneuroma, myofibroma)	1 (high-grade sarcoma NOS)

Conclusions: In conclusion, FNA is useful to triage pediatric spindle cell lesions, in that it can usually exclude more common lymphoid lesions and small round blue cell tumors, thereby directing further management. However, obtaining sufficient material for full characterization with ancillary studies can be difficult, and thus, maximizing cell block material or using concurrent core biopsy can be helpful. Neoplasms that are particularly difficult to diagnose on FNA due to low cellularity were hemangioma and osteosarcoma.

1925 Thyroid Carcinoma in Children and Adolescents: An Institutional Review
NTT Can, T Antic, JB Taxy. University of Chicago, Chicago, IL; NorthShore University HealthSystem, Evanston, IL.
Background: Papillary thyroid cancer (PTC) is the most common thyroid malignancy in children. The diffuse sclerosing (DSV) and cribriform morular (CMV) variants have specific clinical and pathologic associations. DSV is associated with thyroiditis, diffuse growth pattern, and *RET* mutations; while CMV is associated with familial adenomatous polyposis (FAP), a gross mass, and *APC* mutations. This study reviews pediatric thyroid carcinomas.
Design: The files at University of Chicago yielded 43 thyroid carcinomas (total or partial thyroidectomy specimens) in patients <20 years from January 2005 to October 2012.
Results: There were 34 total and 9 partial thyroidectomies among 11M:32F (ages 7-20 years; mean: 16.2 years). PTC distribution was as follows: 18 classic, 15 DSV, 4 follicular variant, and 2 CMV. Other subtypes of thyroid carcinoma included 2 minimally invasive follicular, 1 medullary, and 1 Hurthle cell carcinoma. DSV cases were multicentric (11 cases) with both diffuse growth (3 cases) and mass formation (12 cases), squamous metaplasia (11 cases), psammoma bodies (14 cases), and background thyroiditis (15 cases). In CMV cases, there was the addition of cribriform proliferations without background thyroiditis. One CMV case was sporadic (without β-catenin nuclear positivity by immunohistochemistry); the other was FAP-related with β-catenin nuclear positivity by immunohistochemistry and confirmed germ-line *APC* mutation. When compared with classic PTC, DSV was more frequently associated lymph node metastases (p<0.001) and advanced TNM (III or IV) stage (p=0.004). The only death in this series occurred in a patient with DSV.
Conclusions: This series shows DSV as the major PTC subtype in the pediatric group. Though diffuse growth has been reported as characteristic of DSV, 12 cases exhibited a gross mass. Squamous metaplasia, psammoma bodies, background thyroiditis, and multicentricity were common histologic features. The histological features shared between DSV and CMV suggest they may be part of a morphologic spectrum. In the absence of cribriform proliferations, DSV and CMV can appear morphologically identical. Molecular diagnostics may aid in distinguishing these two entities. While the association between CMV and FAP is well known, some cases of CMV may be sporadic. An example of each was encountered in this series. DSV has been previously identified as an aggressive PTC variant and accounted for the only death in this series. Histologic subtype and tumor stage may be significant determinants of the biologic behavior of thyroid cancer in children.

1926 MiR-125b in Pediatric Fibroblastic Tumors
R Cappellesso, F Simonato, L Iaria, A Fassina, L Ventura, A Zin, R Alaggio. University of Padova, Padova, Italy.
Background: Intermediate and malignant fibroblastic-myofibroblastic tumors are an important group of malignancies that includes variants of fibrosarcoma, such as congenital infantile fibrosarcoma (CIFS), primitive myxoid mesenchymal tumor of infancy (PMMTI), and undifferentiated sarcoma (US). To date, little is known about the involvement of microRNAs in these tumors. MiR-125b regulates cellular quiescence (reversible cell-cycle arrest) and has been reported to be up-regulated in quiescent fibroblasts. However, the down-regulation of miR-125 has been reported in several tumors where it exhibits tumor suppressor properties, while its over-expression in other malignancies has been related to oncogene functions.
Design: MiR-125b expression was analysed by using qRT-PCR in formalin-fixed paraffin-embedded specimens of 6 CIFSs with known ETV6-NTRK3 gene fusion, 6 sarcomas without this genetic alteration (3 PMMTIs and 3 USs), and 7 cutaneous scars (negative controls). Statistical analysis was done using Student *t*-test.

Results: qRT-PCR analysis highlighted that miR-125b was more expressed (*p*=0.0154) in the group of PMMTIs and USs than in cutaneous scars and showed an upward trend (*p*=0.0859) in these tumors in comparison with CIFSs. The amounts of this miRNA were similar (*p*=0.3027) in CIFSs and negative controls.

Conclusions: Pediatric sarcomas lacking the ETV6-NTRK3 gene fusion show a significantly higher expression of miR-125b compared to controls. Moreover, the upward trend of expression in PMMTI in comparison with CIFS supports their distinction. Whether the expression of miR-125b is related to the maintenance of a "primitive" status of the neoplastic cells or to its oncogenic properties should be investigated in further studies.

1927 Colorectal Cancer in Hereditary Leiomyomatosis and Renal Cell Carcionoma Syndrome (HLRCC)

A Castillejo, AB Sanchez -Heras, C Egoavil, C Esquembre, M Castillejo, A Martinez -Canto, M Trigueros, JI Lopez, I Blanco, C Alenda, FI Aranda, J Soto. Elche Hospital, Genetic Counselling in Cancer Unit, Molecular Genetics Laboratory, Elche, Spain; Alicante Hospital, Pathology, Pediatric Medicine, Alicante, Spain; Hospital de Cruces, Barakaldo, Spain; Institut Catalá d´Oncología, Barcelona, Spain.

Background: HLRCC is a hereditary condition predisposing for development cutaneous and uterine leiomyomas and/or kidney cancer. However the clinical phenotype is uncompletely defined and new unexpected tumors are emerging. HLRCC is caused by germline mutation of *FH* gene. We provide new insights into the clinical, pathological and molecular phenotype of HLRCC.

Design: Family suspicious of HLRCC. Index case: male, 10 y/o with unilateral and multifocal renal tumor (RCC). His father had cutaneous leiomyoma at 46y/o and diagnosed of colorectal cancer (CRC) at 50y/o. Germline genetic analysis was performed. Comprehensive immunohistochemical and molecular characterization of renal and CRC was assessed.

	RCC	CRC
Clinical and pathological features	Unilateral (right) and multifocal RCC	Adenocarcinoma. Two adenomas. Liver metastasis.
Protein expression	Positive: AMARC, EpCAM, B-catenin, Vimentin, CK18. Focal positive: CK19, CD10, RCC, Ki67 (3%). Negative for: FH, CK5/6,7,15,17,20, CD117	Positive for: p53, B-catenin, Ki67 (84%). Negative for FH
Molecular features	BRAF WT, KRAS WT, MSS, No methylation phenotype. LOH at FH	BRAF WT, KRAS mut: G12D, G12R, MSS, Methylation phenotype (3/8): (IGF2, NEUROG1, RUNX3). LOH at FH

Results: RCC: six tumors (0.3-4.3 cm) on right kidney with histology of RCC, non capsulated, no clear cells neither microcalcifications, scarce mitosis and areas of necrosis. CRC: well differentiated adenocarcinoma on distal colon invading adipose perivisceral tissue, metastatic node involvement (5/10) plus two low-grade dysplastic adenomatous polyps and three liver metastasis: T3N2M1. Genetic analysis by sequencing *FH* gene, revealed the presence of a heterozygous pathogenic mutation (c.1118A>G; p.Asn373Ser). Loss of FH protein expression was found in both, RCC and CRC tumours. *FH* allelic loss was evidenced in both tumors by MLPA and RT-PCR methods. We detected two *KRAS* mutations in CRC (G12D/G12R) suggesting molecular heterogeneity. These results lead us to conclude that biallelic inactivation of *FH* gene is observed in both type of tumors suggesting a previously unreported role in colorectal carcinogenesis.

Conclusions: Our findings suggest that individuals diagnosed with HLRCC are at risk for CRC and surveillance should be recommended. More extensive analysis of cohorts of patients with HLRCC will provide information on genotype–phenotype correlations that might influence clinical management.

1928 Evaluation of UBE4B Expression in Neuroblastoma- Genetic and Morphological Stratification Group

R Guo, AM Major, EF Hollingsworth, D Lopez-Terrada, P Zage. Texas Children's Hospital/Baylor College of Medicine, Houston.

Background: Neuroblastomas (NBs) are one of the most common solid tumors in infancy and early childhood. Exploring novel molecular biomarkers is a prerequisite for better risk stratification and prediction of treatment response. The *UBE4B* gene encodes an E3/E4 ubiquitin ligase involved in the degradation of growth factor receptors (GFRs) and is located in the 1p36 region. 1p36 microdeletion and reduced *UBE4B* gene expression have been associated with poor outcome in NB patients, suggesting that UBE4B-mediated GFR degradation may be critical for neuroblastoma pathogenesis. Previous studies were based on mRNA and Western blotting analysis of frozen tissue specimens, and without addressing potential tumor heterogeneity, often a striking feature of NB. In this study, we evaluated UBE4B expression by immunohistochemistry (IHC) using formalin-fixed paraffin embedded (FFPE) tissue NB specimens, and correlated these finding with other genetic markers including *MYCN* gene amplification, and 1p36 microdeletion by fluorescence in situ hybridization (FISH).

Design: We reviewed 35 archival NB cases diagnosed at our institution. FFPE specimens were used for IHC and FISH. The anti-UBE4B antibodies were purchased from Abcam. A commercially available FISH probe was used for 1p36 microdeletion (Vysis 1p36 Microdeletion region probe, Abbott Molecular). *MYCN* gene amplifications were analyzed on these cases using our clinically validated FISH assays.

Results: Of the 35 NB cases, 21 cases were poorly or undifferentiated (PD/UF) and 8 cases differentiating. Among the PD/UF cases, tissue from 3 cases was from metastases to liver or bone marrow. UBE4B expression was diffusely or focally reduced in 18 cases (16 cases diffuse, 1 case focal and 1 case in PD component of intermixed type) (51.4%). Reduction of UBE4B expression was only seen in PD/UF NBs or the PD component of intermixed NBs. 4 of these cases demonstrated *MYCN* gene amplification (22.2%).

Of the 17 cases without reduced UBE4B expression, 4 cases are *MYCN* gene amplified (24%). 22 cases were analyzed for 1p36 microdeletion by FISH, with 3 of them showing single copy of chromosome 1p (13.6%). All of the 3 cases were *MYCN* gene amplified.

Conclusions: Reduced UBE4B expression is a common event in neuroblastoma tumors. IHC for UBE4B is a reliable approach to addressing heterogeneity of neuroblastoma. In our study panel, reduced UBE4B expression in NB is associated with poorly differentiated histology.

1929 The Diagnostic Utility of Acute Histologic Chorioamnionitis at Term in Neonatal Sepsis

L Hakima, Y-A Tseng, AJ Yee, S Islam, N Hanna, P Khullar. Winthrop University Hospital, Mineola, NY.

Background: Acute Histologic Chorioamnionitis (HC) due to its known association with poor maternal and perinatal outcome is one of the most important findings in placental pathology. The clinical significance of HC in full term infants, however, remains controversial with respect to treatment and follow up. Recent literature suggests poor diagnostic utility of HC at term and a non-infectious etiology. In this study, we investigate the association and predictive ability of HC, funisitis, and Chorionic Plate Vasculitis (CPV) in diagnosing early onset sepsis in full term infants.

Design: This was a retrospective study of symptomatic full term infants with presumed sepsis admitted to NICU from 2008-2011(n= 221). Laboratory markers for sepsis (CRP ≥ 10, immature to total neutrophil (IT) ratio ≥ 0.20), duration of antibiotic treatment (≥ 7 days), and blood culture results were obtained to confirm clinical sepsis. Placenta histologic findings of HC, funisitis, and CPV were reviewed and staged according to the Redline classification system.

Results: HC was present in all 221 patients, of which 96 (43%) were septic and 125 (56%) were non-septic. There was a significant trend between increasing stages of HC and sepsis (P = 0.005). Funisitis was present in 60 (63%) of septic patients and 65 (52%) of non-septic patients. There was no trend between increasing stages of funisitis (stages 1 and 2) and sepsis. One case with funisitis stage 3 was excluded from analysis. CPV was present in 66 (69%) of septic patients and 66 (53%) of non-septic patients (P = 0.01).

Conclusions: The presence of HC or funisitis at term, although significant, does not accurately differentiate between septic and non-septic patients. There is a significant trend between increasing stages of HC and sepsis. Chorionic plate vasculitis is also significantly associated with sepsis. Therefore, placenta histologic findings of HC, funisitis, and CPV in full term infants, although significant, are not specific and should not be used as independent markers to diagnose sepsis in order to prevent unnecessary antibiotic treatment.

1930 Progression of a Mixed Epithelial Stromal Tumor Harboring DICER1 Mutations

KA La Fortune, DA Hill, HP Cathro, RD LeGallo. University of Virginia, Charlottesville, VA; Children's National Medical Center, Washington, DC.

Background: Germline inactivating DICER1 mutations predispose patients to a broad range of rare benign and malignant neoplasms, most notably pleuropulmonary blastoma (PPB) and cystic nephroma (CN). While PPB harbors the potential to progress from a purely cystic lesion to anaplastic solid sarcoma, CN is considered benign with no malignant potential. We report a case of a multiloculated renal epithelial stromal tumor that recurred as a high-grade sarcoma harboring biallelic DICER1 mutations.

Design: A 20-year-old woman presented to the emergency department with gross hematuria and flank pain. Renal ultrasound demonstrated a multiloculated mass arising from the left renal parenchyma most consistent with a CN. She underwent partial nephrectomy and the lesion was diagnosed as a mixed epithelial and stromal tumor. Eleven months post-resection, she returned with acute right adnexal tenderness. MRI revealed a heterogeneously enhancing soft-tissue mass of the lower pelvis that was biopsied to reveal a high-grade spindle cell sarcoma. Due to the lesion's similarities to a CN, the possibility of a DICER1 mutation was raised. Frozen tissue from the sarcomatous resection specimen was submitted for mutation analysis.
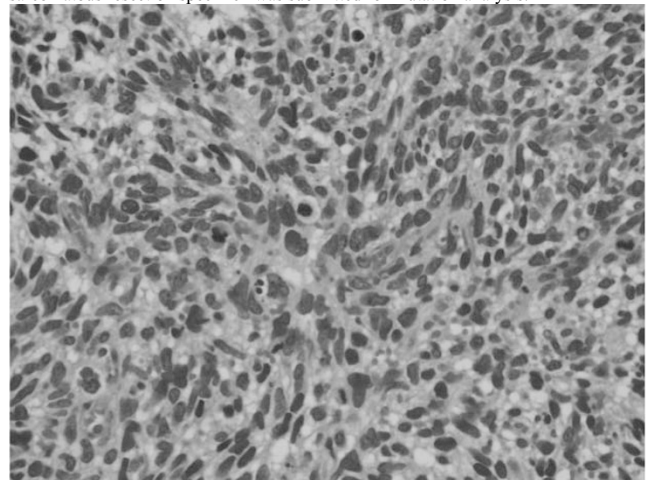
Results: Biallelic DICER1 mutations were identified from tumor-derived DNA. The first mutation introduced a stop codon for Arginine (Arg745X) and the second mutation introduced a missense mutation substituting lysine for glutamine (Glu1813Lys). Germline DNA was not available for analysis.

Conclusions: The DICER1 mutations identified in this sarcoma are similar to reported germline mutations and secondarily acquired mutations in patients with PPB and related tumors. While sporadic DICER1 mutations are increasingly recognized in a low percentage of malignancies including rare cases of embryonal rhabdomyosarcoma and even less frequently nephroblastoma, our case does not represent either of these categories. We report the first case of a DICER1 mutation in a malignant cystic renal tumor, which raises the possibility of sarcomatous transformation of CNs similar to the biologic progression of PPB.

1931   Performance Testing of the Bethesda System for Reporting Thyroid Cytopathology in Children
P Lokhandwala, D Zander, N Williams, H Mani, M Walls, C Abendroth. PSHMC, Hershey, PA.
Background: The Bethesda System for Reporting Thyroid Cytopathology (TBSRTC) has received limited performance testing in pediatric populations. We completed a retrospective cytologic-histologic correlative analysis of all pediatric thyroid FNAs performed in the last 3.5 years at our tertiary care medical center to evaluate the ability of Bethesda System classification to predict histology.
Design: A search of our CoPath database from March 2010 to August 2013 yielded 32 thyroid FNAs obtained from 23 children aged 10 to 18 years. This represented 2% of all thyroid FNAs performed at our institution over this time period. The medical records were searched for subsequent surgical pathology specimens and the histologic diagnoses were compared with the FNA interpretations.
Results: A tabulation of thyroid FNA interpretations and subsequent histology is shown below. Although this study is limited by the relatively small number of cases in each diagnostic category, surgical follow-up of cases interpreted as suspicious or positive for malignancy yielded a malignant neoplasm in all cases (100% sensitivity, PPV=100%). Eight patients undergoing surgery after an FNA interpretation of Non-diagnostic, Benign, AUS/FLUS, or FN/SFN received histologic diagnoses that were non-neoplastic or benign neoplasms. After first FNA 17 of 32 patients were triaged to clinical follow-up only, while 3 Benign and 2 Non-Diagnostic cases were followed-up with a repeat FNA that resulted in four Benign and one suspicious for follicular neoplam.

Category	FNA (N)	FNA (%)	Surgery (N)	Histology - Non-Neoplastic	Histology - Benign Neoplastic	Histology - Malignant
Non-diagnostic	5	15.6	1	1 (100%)	0 (0%)	0 (0%)
Benign	18	56.3	2	0 (0%)	2 (100%)	0 (0%)
AUS	3	9.4	3	3 (100%)	0 (0%)	0 (0%)
FN/SFN	3	9.4	2	2 (100%)	0 (0%)	0 (0%)
SFM	2	6.3	2	0 (0%)	0 (0%)	2 (100%)
Malignant	1	3.1	1	0 (0%)	0 (0%)	1 (100%)
Total	32	100.0	11	6 (60%)	2 (20%)	3 (30%)

(AUS=Atypia of undetermined significance, FN/SFN=Follicular neoplasm/suspicious for follicular neoplasm, SFM=Suspicious for Malignancy).
Conclusions: Thyroid FNAs are uncommonly performed in children, probably because of the low incidence of thyroid malignancy in this age group. Thyroid FNA had excellent sensitivity for malignancy. Intermediate categories (AUS/FLUS) and FN/SFN) were associated with subsequent benign histology, suggesting that these categories may need different management strategies in children as compared to adults, although larger/multicenter studies are needed to further validate this.

1932   Early Post-Partum Diagnosis of Intra-Amniotic Infection by Frozen Section
ER Mahe, J Hamid, JW Jansen, J Bourgeois, J Arredondo. Calgary Lab Services, Calgary, AB, Canada; McMaster University, Hamilton, ON, Canada; Cambridge Memorial Hospital, Cambridge, ON, Canada.
Background: Chorioamnionitis and funisitis represent histopathological manifestations of intraamniotic infection. These diagnoses follow the identification of neutrophilic infiltration of the fetal membranes or umbilical cord, respectively. Although frozen section diagnosis of intra-amniotic infection has been suggested as a viable technique in the older literature, it has not yet been rigorously studied or validated for routine clinical use.
Design: Forty-nine samples of frozen umbilical cord and placental membrane tissue were included in the study. Frozen sections of each were cut at 5 um and stained using routine frozen-section hematoxylin & eosin (H&E) techniques. The remaining tissue was then formalin-fixed and parafin-embedded to produce permanent section slides, also stained with H&E. The frozen section and permanent section slides were blinded and compared by three expert pediatric pathologists individually and then by panel consensus after a delay of several weeks. The grade and stage of neutrophilic inflammation were recorded as per the Redline grading/staging technique.
Results: Frozen sections detected inflammation with a positive likelihood ratio of 2.89 (95%CI 1.27 - 6.58) and a negative likelihood ratio of 0.16 (95%CI 0.059 - 0.43) in umbilical cord sections and a positive likelihood ratio of 2.28 (95%CI 1.22 - 4.27) and a negative likelihood ratio of 0.15 (95%CI 0.046 - 0.47) in placental membrane sections. Goodness-of-fit testing demonstrated a statistically significant correlation between frozen and permanent sections when the full grading and staging system of Redline was used (p<0.001 for both umbilical cord and placental membrane sections). The assessment of frozen sections and permanent sections was not significantly different by kappa-statistic testing (p=0.06).
Conclusions: We have performed, to our knowledge, the first rigorous study of frozen section for the early post-partum diagnosis of intraamniotic infection. We demonstrated that frozen sections of fetal membranes and umbilical cord are accurate in the estimation of the grade and stage of maternal and fetal inflammatory responses. The rapidity by which frozen sections can be performed portends a valuable and accurate diagnostic aid in the early post-partum detection of intra-amniotic infection. Early diagnosis by frozen section may be a valuable ancillary test, perhaps aiding in better outlining early post-partum treatment regimens in births complicated by intra-amniotic infection.

1933   Diffuse and Strong CyclinD1 Immunoreactivity in Clear Cell Sarcoma of the Kidney
J Mirkovic, M Calicchio, C Fletcher, A Perez-Atayde. Brigham and Women's Hospital, Boston, MA; Boston Children's Hospital, Boston, MA.
Background: Distinction of clear cell sarcoma of the kidney (CCSK) from other pediatric renal malignancies, particularly blastema-rich Wilms tumor (WT) and cellular congenital mesoblastic nephroma (CMN) is challenging. No specific immunohistochemical profile has been identified, and diagnosis rests primarily on histopathology. Recently, YWHAE-FAM22 rearrangement, identical to that seen in high-grade endometrial stromal sarcoma (ESS), has been identified in a proportion of CCSK. Since this fusion gene results in overexpression of cyclinD1 in high-grade ESS, we studied the utility of cyclinD1 immunohistochemistry in the differential diagnosis of CCSK.
Design: CyclinD1 immunohistochemistry expression was evaluated in 59 renal tumors: CCSK (14), WT (25), rhabdoid tumor (4), Ewing sarcoma (5), CMN (11) – and 4 neuroblastomas. The pattern of staining was graded as diffuse (>70%), focal (>5% to 70%), or negative. The intensity of staining was graded as strong 3+ (same intensity as mantle cell lymphoma control), moderate 2+, and weak 1+.
Results: All 14 cases of CCSK exhibited diffuse 3+ cyclinD1 nuclear reactivity. In contrast, blastematous WT component exhibited only rare positive nuclei in most tumors (18/20, 2 exhibited focal up to 40%, 2-3+ nuclear staining). The epithelial component of WT ranged from negative to diffusely 3+ nuclear reactivity. Rhabdoid tumors exhibited rare positive cells to focal (up to 30%, 2-3+) nuclear staining. Majority of Ewing sarcomas (3/5) and all neuroblastomas exhibited diffuse 2-3+ nuclear staining. Seven CMN exhibited diffuse 1-3+ nuclear staining and 4 focal (2-3+) nuclear staining.
Conclusions: All CCSK show diffuse 3+ cyclinD1 nuclear staining. CyclinD1 immunohistochemistry helps distinguish CCSK from WT and rhabdoid tumor, but not from neuroblastoma, most renal Ewing sarcomas or most CMN. Our data indicate that CyclinD1 inhibitors may potentially be useful in targeted therapy for CCSK.

1934   Differential Diagnosis of Small Round Cell Tumors by Transcriptome-Wide Expression Profiling
AP Mitra, D Haydel, SA Mitra, L Wang, TJ Triche. University of Southern California, Los Angeles, CA; Children's Hospital Los Angeles, Los Angeles, CA.
Background: Differential diagnosis of malignant small round cell tumors (SRCTs) can be challenging due to their undifferentiated character. Their primitive histopathology often renders identification of morphological features difficult and therefore, no definitive diagnosis may be possible. This is important in pediatric SRCTs as a variety of therapeutic approaches are used for distinct tumor types based on a patient's risk. This study sought to identify diagnostic signatures for a variety of SRCTs using transcriptome-wide expression profiling.
Design: RNAs were extracted from 115 prospectively-obtained, frozen primary pediatric SRCT specimens and profiled on Affymetrix Human Exon 1.0 ST arrays. These comprised of Ewing sarcoma (n=10), neuroblastoma (n=10), *PAX-FKHR* fusion-negative rhabdomyosarcoma (F-RMS, n=20), *PAX-FKHR* fusion-positive rhabdomyosarcoma (F+RMS, n=19), lymphoma (n=10), Wilms tumor (n=10), clear cell sarcoma (n=7), rhabdoid tumor (n=9), medulloblastoma (n=10), and osteosarcoma (n=10). Binary screens were performed for each tumor type to identify diagnostic probe selection regions (PSRs). Selected PSRs were combined as a signature, and its diagnostic potential was assessed by k-nearest neighbor algorithms and unsupervised hierarchical clustering.
Results: Expressions of 1,393,765 PSRs corresponding to thousands of transcripts were analyzed for each candidate tumor type. Binary screens identified hundreds of diagnostic PSRs corresponding to annotated and unannotated transcripts for each SRCT type. To limit signature size, the top six PSRs were chosen for each tumor type. Between 17% and 83% of features in each signature represented non-exonic content. Unsupervised hierarchical clustering demonstrated the ability of each signature to diagnose the corresponding tumor by binary and multiplex analyses. Discrimination analysis showed that signatures for Ewing sarcoma, neuroblastoma, F+RMS, lymphoma and osteosarcoma were the best performing and most exclusive. Overall, each tumor signature had robust diagnostic potential (binary discrimination, all p<0.0001).
Conclusions: Using pediatric SRCTs as an example, this study illustrates that transcriptome-wide analysis can reveal potential transcripts that can robustly diagnose malignancies that pose a histological challenge. Such concise genomic signatures can be translated to clinical assays for routine diagnostic implementation.

1935   Whole Native Liver Explant Pathology in Pediatric Liver-Intestinal Transplant Recipients Who Received Omegaven® Lipid Emulsion Therapy
R Shen, C Matsumoto, SS Kaufman, B Kallakury. Medstar Georgetown University Hospital, NW Washington, DC; Medstar Georgetown Transplant Institute, NW Washington, DC.
Background: Many infants on parenteral nutrition for intestinal failure will develop parenteral nutrition associated liver disease (PNALD). It is the most severe complication of long-term parenteral nutrition. These infants present with cholestasis, which may be followed by progressive fibrosis, eventually leading to cirrhosis. The pathophysiology of PNALD is unclear. Reports have indicated that substitution of conventional soy oil-based lipid emulsions with a product based on fish oil that is rich in omega-3 polyunsaturated fatty acids, Omegaven© reverses hyperbilirubinemia in these patients. More recent reports, based on biopsy specimens, have not shown an improvement

in hepatic fibrosis despite reversal of hyperbilirubinemia with Omegaven©. Detailed pathologic findings of whole explanted native livers in children who have undergone a combined liver-intestine transplant on Omegaven therapy have not been reported.

Design: Explanted whole native livers from seven patients who have received Omegaven© emulsion as parenteral nutrition therapy in the pretransplant period were evaluated. Histological features including degree of inflammation, fibrosis, steatosis, cholestasis and portal bile duct proliferation were semiquantitatively scored according to established criteria.

Results: The pathological features of the seven native liver explants are summarized in the following table.

Features	Pt. 1	Pt. 2	Pt. 3	Pt. 4	Pt. 5	Pt. 6	Pt. 7
Protal inflammation(0-4)	1	1	1	1	1	2	1
Bile Duct Proliferation(0-3)	1	3	1	1	1	3	1
Interface Hepatitis(Yes/No)	No	No	No	No	No	Yes	No
Steatosis(0-3)	1	1	1	0	1	0	0
Cholestasis(0-3)	1	3	2	0	0	2	0
Lobular Hepatitis(Yes/No)	No	No	No	No	No	No	No
Clear Cell Change(Yes/No)	Yes	Yes	No	No	No	Yes	No
Fibrosis Stage(0-4)	3	3	3	4	4	4	3

All patients had resolution of hyperbilirubinemia while on Omegaven© therapy. Six of the seven patients(86%) showed minimal active inflammation. All cases showed bridging fibrosis and 3 of them(42.9%) had established cirrhosis (stage 4).

Conclusions: Pediatric intestinal transplant recipients who received Omegaven© emulsion therapy showed minimal to mild inflammation, mild cholestasis and yet advanced fibrosis in their explants. The reason for this discordance is unclear as a chronic inflammatory state has generally been considered a precursor to advanced hepatic fibrosis. In this series, while Omegaven® emulsion therapy may have improved degree of inflammation and cholestasis, progression to severe fibrosis and cirrhosis was not altered.

1936   Clinical Co-Morbidities, Ablative Site Placental Calcification, and Vascular Remodeling in Twin-to-Twin Transfusion Syndrome with and without Selective Fetoscopic Laser Photocoagulation (SFLP)
SE Starnes, P Fitchev, C Thorpe, E Vlastos, S Mehra, M Cornwell, SE Crawford. Saint Louis University School of Medicine, St. Louis, MO.

Background: Twin-to-twin transfusion syndrome (TTTS), imbalanced shunting of blood from one twin to the other via placental vascular anastomoses, complicates approximately 10 to 15% of monochorionic pregnancies and carries a high risk of fetal mortality. The current treatment of choice for TTTS is selective fetoscopic laser photocoagulation (SFLP) and ablation of the vascular anastomoses. Recurrence of TTTS after SFLP occurs in up to 16% of cases and is associated with an adverse outcome. Previous studies of placental pathology in TTTS cases have primarily focused on angioarchitecture in placentas not treated by SFLP with scant evaluation of other microscopic findings.

Design: Charts of 9 cases of twin pregnancies affected by TTTS were reviewed; 6 underwent SFLP and 3 had no intervention. All cases were assessed by *ex vivo* vascular injection studies with gross and microscopic evaluation. Sections were taken at SFLP sites, remote from sites, and of any grossly abnormal regions. Studies including immunohistochemistry were performed to highlight the vasculature (CD31, smooth muscle actin, endothelin) and to confirm calcium deposition.

Results: Of TTTS cases (n=9), mean maternal age was 24 yrs (range 20-32 yrs). For this young age group, there was a high rate of co-morbidities including obesity, diabetes, biliary disease, smoking, and hematopoietic abnormalities. Fetal demise of one twin occurred in 67% (2/3) of the untreated group, but in those with SFLP, the rate was only 33% (2/6). Vascular studies showed residual anastomoses in one case. There was abnormal umbilical cord insertion in 44% (4/9). Histologic analysis revealed vascular pathology including intravascular calcifications in 67% (6/9), two of which had no SFLP. In 6/7 cases with SFLP treatment, fine concentric calcifications surrounded areas of villous fibrosis underlying SFLP sites and in 3/7, there was a wedge-shaped infarct subjacent to the SFLP site.

Conclusions: This cohort of women with gestations complicated by TTTS was young, with a high number of co-morbidities, especially metabolic (30%). There was accelerated mineralization of choriovillous vasculature in TTTS placentas regardless of SFLP status, suggesting a new disease association. The wedge-shaped infarcts associated with SFLP sites indicate that superficial chorionic intervention can significantly alter subjacent placental perfusion.

Pulmonary Pathology

1937   ALK Rearrangement Detection in NSCLC: Comparison between Fluorescent In Situ Hybridization, Immunohistochemistry, and MassARRAY Based Method
G Ali, A Proietti, S Pelliccioni, C Niccoli, C Lupi, E Sensi, R Giannini, N Borrelli, M Menghi, A Chella, A Ribechini, F Cappuzzo, F Melfi, M Lucchi, A Mussi, G Fontanini. Unit of Pathological Anatomy, Azienda Ospedaliera Universitaria Pisana, Pisa, Italy; University of Pisa, Pisa, Italy; Diatech Pharmacogenetics, Pisa, Italy; Unit of Pneumology, Azienda Ospedaliera Universitaria Pisana, Pisa, Italy; Endoscopic Section of Pneumology, Azienda Ospedaliera Universitaria Pisana, Pisa, Italy; Istituto Toscano Tumori, Ospedale Civile, Livorno, Italy; Unit of Thoracic Surgery, Azienda Ospedaliera Universitaria Pisana, Pisa, Italy.

Background: *EML4-ALK* translocation has been described in a subset of patients with non-small cell lung cancer (NSCLC) and has been shown to have oncogenic activity. Fluorescent in situ hybridization (FISH) is used to detect *ALK*-positive NSCLC, but it is expensive, time-consuming and difficult for routine application. For these reasons, we evaluated the potential role of immunohistochemistry (IHC) as a screening tool to identify candidate cases for FISH analysis and for ALK inhibitor therapy in NSCLC. To verify the mRNA expression of EML4-ALK, we used a MassARRAY method in a small subset of patients.

Design: We performed FISH and IHC for *ALK* and mutational analysis for *EGFR* and *K-ras* in 523 NSCLC specimens. We conducted IHC analysis with the monoclonal antibody D5F3 and a highly sensitive detection system. We also performed a MassARRAY-based analysis in a small subset of 11 samples to detect *EML4-ALK* rearrangement.

Results: Of the 523 NSCLC specimens, 20 (3.8%) were positive for *ALK* rearrangement by FISH analysis. *EGFR* and *Kras* mutations were identified in 70 (13.4%) and 124 (23.7%) out of 523 tumor samples, respectively. *ALK* rearrangement, *EGFR* and *Kras* mutation were mutually exclusive. Out of 523 analyzed tumor samples, 18 (3.4%) were ALK positive by IHC. 18 samples had concordant IHC and FISH results, and 2 *ALK* FISH-positive cases failed to show ALK protein expression. In these two discrepant cases, MassARRAY confirmed the absence of EML4-ALK expression.

Conclusions: In conclusion, our results show that IHC may be a useful technique for selecting NSCLC cases to undergo *ALK* FISH analysis.

1938   Necrosis and Nuclear Grade Are Predictors of Overall Survival in Epithelioid Malignant Mesotheliomas (EMM)
V Ananthanarayanan, S McGregor, Q Arif, D Hadi, M Alikhan, W Vigneswaran, T Krausz, AN Husain. University of Chicago, Chicago, IL.

Background: Mesotheliomas with epithelioid histology are considered to have a better prognosis than biphasic or sarcomatoid mesotheliomas. A recently published article demonstrated the prognostic importance of nuclear grading in predicting survival in patients with epithelioid diffuse malignant pleural mesothelioma (Kadota K etal. Mod Path, 2012, 25, 260-71). The current study was undertaken to determine the usefulness of this grading system.

Design: We examined all resected/ debulked cases of pleural epithelioid malignant mesothelioma (EMM) from 2006 to 2010 after appropriate institutional review board approval. H&E slides were reviewed and nuclear grade was computed combining nuclear pleomorphism and mitotic rates into a semi-quantitative score of grades I-III using Kadota *et al's* grading system. The presence or absence of any necrosis and the predominant patterns of growth were also evaluated. Overall survival (OS) was used as the primary end point for all data analysis. Data were examined using Pearson's Chi-square test, proportional hazards regression and log rank tests within STATA 11® (StataCorp, Texas).

Results: A total of 33 patients (6:1 male: female ratio) with 27 low grade (12 Grade I and 15 Grade II) and 6 high grade (Grade III) EMMs were analyzed. Grade was significantly associated with necrosis (pX^2=0.032). A total of 9 deaths were noted among 26 patients with a mean follow up duration of 40 months (range 6-86). Univariate analyses showed that necrosis impacted OS ($p_{log-rank}$=0.01, figure 1b). A predominant solid pattern was marginally associated with OS ($p_{log-rank}$=0.06) while age did not impact outcome (p=n.s.). Furthermore, nuclear grade as a two-tier (HR= 8.50, 95% CI=1.40, 51.50, figure 1a) as well as three-tier system (HR=3.77; 95% CI=1.17-12.17) impacted outcome significantly.
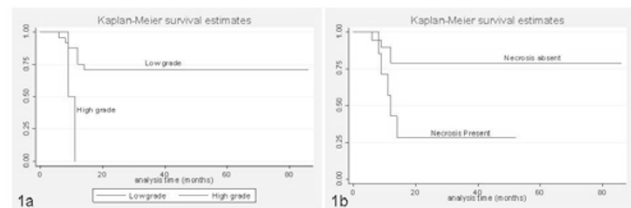
Conclusions: This study performed on a limited sample size emphasizes the importance of examining nuclear grade, patterns of growth and presence or absence of necrosis while evaluating resection specimens of EMM. Multivariate analyses of a larger dataset will clarify the impact of these findings.

1939   Thoracic Epithelioid Vascular Tumors: Prognostic Factors and Usefulness of WWTR1-CAMTA1 Fusion in the Distinction of Epithelioid Hemangioendotheliomas and Angiosarcomas
TA Anderson, WD Travis, CR Antonescu. Memorial Sloan-Kettering Cancer Center, New York, NY.

Background: Epithelioid vascular tumors are a heterogeneous group of tumors that encompass a morphologic spectrum between low and intermediate grade (G1 and G2) epithelioid hemangioendotheliomas (EHE) and high grade (G3) epithelioid angiosarcomas (EA). A WWTR1-CAMTA1 fusion gene has been previously reported in conventional EHEs of various sites; however, only few intrathoracic cases have been studied.

Design: 49 thoracic epithelioid vascular tumors were obtained from the case files at our institution and personal consultations. The clinical course, histologic features and immunohistochemistry (IHC) were reviewed. Fluorescence in-situ hybridization (FISH) analysis for WWTR1 and CAMTA1 gene rearrangements were performed on 30 cases.

Results: There were 36M and 13F with EHE: G1 (n=12) and G2 (n=24) and EA: G3 (n=13). Presentation was exclusively thoracic (n=33), multiorgan including lung (n=14) and metastatic to lung from extrathoracic sites (n=2). The thoracic tumors presented in the pleura (n=19), lung (n=23), mediastinum (n=5), and superior vena cava (n=1). CAMATA1 rearrangements were found in 16/17 (94%) G2, 5/9 (56%) G1 and 0/4